This is the peer reviewed version of the following article:

V. Carević and I. Ignjatović, “Influence of Loading Cracks on the Carbonation Resistance of RC elements”, Construction and Building Materials, vol. 227, pn. 116583, Dec. 2019.

https://doi.org/10.1016/j.conbuildmat.2019.07.309

Influence of Loading Cracks on the Carbonation Resistance of RC elements

Vedran Carević[1*], Ivan Ignjatović [1]

[1]*University of Belgrade, Faculty of Civil Engineering, Department for Materials and Structures, Bulevar kralja Aleksandra 73, 11000 Belgrade, Serbia*

[*] Corresponding author

E-mail address: vedran@imk.grf.bg.ac.rs

Fax: +381 11 3218 253

Tel: +381 64 0720 865

Abstract

In reinforced concrete (RC) structures, carbonation induced corrosion is one of the most significant durability issues. A very important factor that affects the carbonation process is the appearance of cracks in RC structures. According to the current state of the art, cracks have not yet been considered as a parameter in carbonation models which are used for defining the service life of concrete structures. The main objective of this research is to analyse the influence of cracked concrete cover as reinforcement protection. The analysis was carried out using own experimental results and the application of available standards and novel predictions regarding carbonation depth. For that purpose, prismatic RC samples without cracks and with different crack widths (0.05, 0.10, 0.15, 0.20 and 0.30 mm) were made and subjected to accelerated carbonation. The influence of carbonation depth on the corrosion of cracked and uncracked samples was analysed by observing the reduction of the reinforcement cross section. The compressive and tensile stress influence on carbonation resistance was also evaluated. The conducted analysis showed that even with low crack widths (0.05 mm) the maximum carbonation depth was significantly higher compared with uncracked samples. It was also shown that reduction in the reinforcing bar cross section after 28 days of exposure to 2% CO_2 was between 0.05% and 0.13%, depending on the crack width. The results showed that compressive stress increase had no significant effect in the carbonation depth of samples.

Keywords

Crack width; Carbonation; Corrosion; Accelerated test; Service life

1. Introduction

Today, reinforced concrete (RC) is one of the most widely used construction materials. Concrete is usually considered as a building material which possesses good durability properties. Although different deterioration mechanisms can lead to the degradation of the concrete itself, reinforcement corrosion is by far the biggest durability issue for RC structures. In RC structures, reinforcement is physically and chemically protected by the surrounding highly alkaline concrete environment and a thin oxide layer – the passivation layer [1]. If the pH value drops below approximately 9.5, the reinforcement passivation layer breaks down (depassivation) and the corrosion of reinforcement can start. One of the most important depassivation processes in RC structures is carbonation. It represents the process of cement matrix neutralization that leads to the decrease of concrete pH value (from 13 to below 9), which reduces the chemical protection of reinforcement. Therefore, good protection of reinforcement is obtained with adequate concrete cover depth depending on the exposure conditions.

The carbon dioxide (CO_2) from the atmosphere penetrates through the concrete pores, dissolves in the pore solution, reacts with the calcium hydroxide ($Ca(OH)_2$) or hydrated calcium silicate (C-S-H) and produces calcium carbonate ($CaCO_3$) crystals [2]. In this way, the chemical balance between the pore solution and hydrates changes. When the CO_2 is dissolved in the pore solution, carbonic acid reacts with the alkalis in the concrete matrix and decreases the concrete pH value. As a consequence, a higher volume of $CaCO_3$ compared with the $Ca(OH)_2$ leads to the decrease in concrete porosity.

There are many factors that affect the carbonation process (CO_2 concentration, relative humidity, temperature, curing conditions and concrete porosity). Since the time required to determine the carbonation depth in natural conditions (CO_2 concentration of approximately

0.03% in rural and 0.3% in urban areas [3]) is measured in years, the usual quantification of the concrete carbonation resistance is done through accelerated carbonation tests. Accelerating the carbonation process is achieved primarily by increasing the CO_2 concentration, which can results in a change in process kinetics [4]. It has been shown that at a concentration of 2% (*fib* Model Code 2010 guidelines [5]) there will be no major difference in the process kinetics [6].

Possibly the most important factor that affects the carbonation process is the appearance of cracks in RC structures. With relatively low tensile strength of concrete, the cracking of structural elements is almost inevitable due to different action effects. Experience with existing structures showed greater carbonation depth at crack positions compared with uncracked parts of structures. Several practical examples of this phenomenon showed corrosion appearance on crack positions [7]. Despite this, cracks have not yet been taken into account as a parameter in carbonation models which are used for defining the service life of concrete structures (e.g. the *fib*Model Code 2010). On the contrary, it is considered that adequate quality of concrete cover and ordinary crack width limitation ensure a sufficiently long service life ($\geq$ 50 years) without extra protection [5]. Depending on the severity of the environment and sensitivity of the structure, this limiting crack width is normally given as a characteristic value (95^{th} percentile) in the range of 0.2 to 0.4 mm [8].

Studies from almost 30 years ago [9,10] concluded that, although the presence of cracks is a risk, their width cannot be directly related to the developed corrosion. However, several studies investigated the phenomenon of CO_2 diffusion in cracked concrete samples [11–16] in the last decade. The results obtained in those studies are shown in Table 1. The term “critical crack width” (Table 1), refers to the crack width which further increases, i.e. accelerates the affects the CO_2 diffusion. Crack widths below the critical values have no influence on

carbonation depth, whereas wider cracks will increase carbonation depth compared with uncracked samples. Obviously, no clear conclusion regarding the impact of the cracks can be drawn. Although there were some arguments that cracks have no effect on carbonation depth [11,12], some experimental results showed that even with small crack widths (up to 0.10 mm) there was a change in the CO_2 diffusion, i.e. in the carbonation depth [13–16]. All defined critical widths in those studies were smaller than the acceptable crack widths defined in the European standard EN 1992-1-1 [8] – for given exposure conditions the maximum crack width is defined as 0.3 mm.

Numerous researchers have also studied the concrete carbonation resistance under compressive load [16–19]. Wang et al. [16] clearly stated that compressive stresses have a positive effect on the concrete carbonation resistance. On the other hand, Tang et al. [18] and Wan et al. [19] concluded that concrete carbonation resistance under compressive load increased at first but then decreased with increasing compressive stress levels. These findings suggest that concrete compressive stress can also be an important parameter in the analysis of carbonation resistance.

Table 1. The influence of crack widths on the CO_2 diffusion

Reference	Method for crack producing	CO_2 conc.	Critical crack width [mm]
Neville (2006) [11]	-	-	no influence
Sillanpää (2010) [12]	notching and splitting	natural	no influence
Alahmad et all (2009) [13]	expansive core	50%	0.01
Torres and Andrade (2015) [14]	three point bending	natural	0.08*
Zhang et all (2011) [15]	embedded steel slices	20%	0.10*
Wang et all (2018) [16]	four point bending	4%	0.10*

*lower crack widths were not examined

As can be seen, the question regarding the influence of crack widths and mechanical loads on the carbonation process is still unanswered. Although there were several studies on this subject, there is still a lack of results for general conclusions on their influence on the CO_2

diffusion and, especially, on carbonation prediction models. For that reason, the analysis of crack width and mechanical load influence on carbonation depth and prediction models is needed.

2. Objectives and Methodology

The main objective of this research is to analyse the influence of cracked concrete cover as s reinforcement protection. The analysis was carried out using own experimental results and the application of available standards and novel predictions regarding carbonation depth. For that purpose, RC samples without cracks and with different crack width were produced and subjected to accelerated carbonation. Beside the influence of cracks, the experiment was designed to enable the analysis of the effect of stresses in concrete (compressive and tensile stresses) on carbonation resistance. The concrete cover can be cracked but also in a compressive stress state which can affect its ability to protect the reinforcement.

The obtained results regarding the carbonation depth of samples with and without cracks measured on the tensioned sample surface (cracked surface) are presented and analysed using the *fib* Model Code 2010 predictions. Since cracks have not yet been considered as a parameter in the *fib* Model Code 2010 carbonation model, the results of cracked and uncracked samples were compared. Finally, the influence of carbonation depth on the corrosion of cracked and uncracked samples was analysed by observing the reduction of the reinforcement cross section area.

3. Experimental program

3.1. Materials and mix design

Ordinary Portland cement concrete was produced and tested. Natural aggregate used in this study was commercially available river aggregate obtained from the Danube River in Serbia divided in three fractions: I (0/4 mm), II (4/8 mm) and III (8/16 mm). It had a bulk density of

2550 kg/m^3 and water absorption of 1.2% after 24 hours. The commercially available blended Portland cement CEM II/A-M (S-L) 42.5R with a specific gravity of 3040 kg/m^3 was used. The proportioning of the concrete mixture was done based on the absolute volume method. Concrete mix design of the tested concrete is shown in Table 2. The mixture was designed to achieve a 90-days compressive strength of 40 MPa (150 mm cube sample) with the slump value after preparation in the range from 80 to 110 mm. The 90-days testing age was chosen because as a part of a larger research involving the use of high volume fly ash concrete, which has not yet been completed. This period enables the development of the pozzolanic reaction in high volume fly ash concrete and provides sufficient time for each concrete to reach its compressive strength potential. Concrete strength was design to ensure concrete class C25/30.

Table 2. Mix proportions of tested concrete

			Natural aggregate		
Concrete	Cement [kg/m^3]	Water [kg/m^3]	I (0/4) [kg/m^3]	II (4/8) [kg/m^3]	III (8/16) [kg/m^3]
NAC	276	175	838.4	558.9	465.8

3.2. Casting, curing and testing of specimens

The concrete was cast in steel moulds, and compacted using a vibrating table. For the compressive strength testing at all ages, 150 mm cube samples were prepared. Carbonation resistance was tested on the 100 x 100 x 500 mm reinforced concrete prisms (Figure 1).

Figure 1. Preparation of the samples for the accelerated carbonation testing

The prismatic samples had a reinforcing bar at the bottom of the sample (Figure 1). High yield, smooth, cold-rolled reinforcing bars were used, with a diameter of 8 mm. An ultimate tensile strength test was carried out and stress-strain relation was recorded during the test (Figure 2). The values for yielding strength and ultimate tensile strength of the bar were 542 MPa and 587 MPa, respectively. Furthermore, the modulus of elasticity (E_s) was determined in the region of linear-elastic behaviour as the stress–strain ratio, giving a value 208.5 GPa.

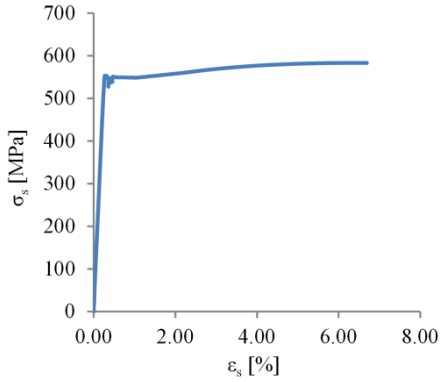

Figure 2. Stress–strain relation of the reinforcing steel bar

After casting, the specimens were covered with wet fabric and stored in a casting room at 20±2^{o}C. They were demoulded after 24 h and the concrete cubes were kept in a water tank until testing while the concrete prisms were covered with a wet fabric and kept in the casting room for additional 6 days. The physical and mechanical properties of the tested concrete are shown in Table 3. The presented results show the mean value of measurements on three samples.

Workability of the tested concrete was in the designed range. The 28-day mean compressive strength obtained on 150 mm cubes was 34.7 MPa, while after 90 days it was 41.5 MPa, which would classify this concrete as class C25/30 according to EN 1992-1-1 [8]. The maximum coefficient of variation (CoV) within any three cubes tested on the same day was 3.4%.

Table 3. Physical and mechanical properties of tested concrete

Property	Mean value	CoV (%)
$\gamma_{c,fresh}$ [kg/m^3]	2345	0.6
$\gamma_{c,hardened}$ [kg/m^3]	2342	0.5
Slump [mm]	110	9.5
$f_{c,7}$ [MPa]	25.8	1.0
$f_{c,14}$ [MPa]	30.2	3.4
$f_{c,28}$ [MPa]	34.7	1.4
$f_{c,90}$ [MPa]	41.5	1.3
$f_{ct,fl,28}$ [MPa]	5.3	0.8
$f_{ct,fl,90}$ [MPa]	6.0	11.7
$E_{c,28}$ [GPa]	31.9	1.7
$E_{c,90}$ [GPa]	32.8	0.6

At the age of 90 days, three point bending was applied on the prism samples to induce cracks. The experimental setup is shown in Figure 3.

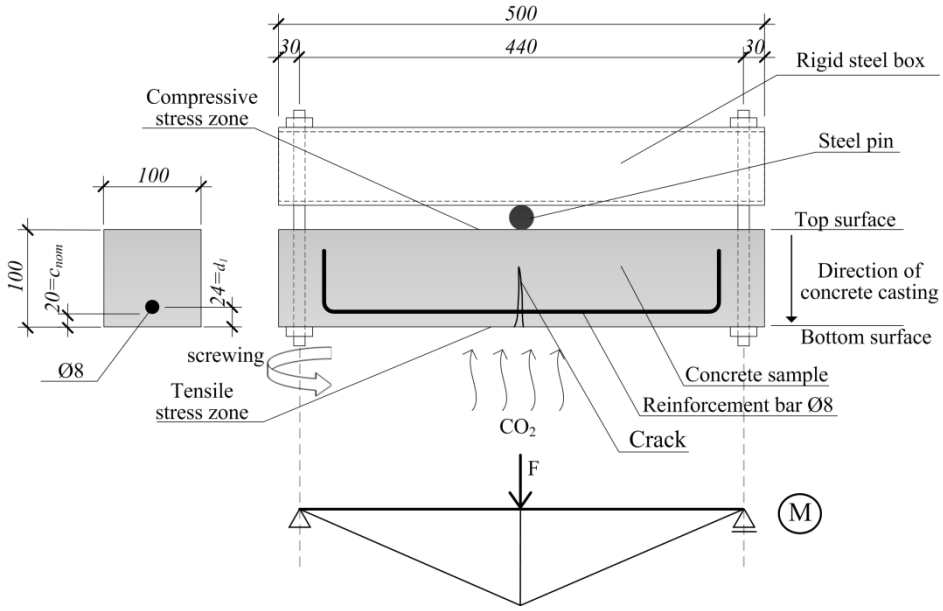

Figure 3. Experimental setup

The rigid steel box was placed on the top of the sample to act as a support for the whole system. The force is applied using a torque wrench and a steel pin which is set in the middle of the span, between the concrete element and a steel box. Having in mind that a three point bending test was used and the shape of the bending moment diagram, one crack was expected

to occur at the point of the maximum bending moment. After the surface crack width reached a desired value, application of force using a torque wrench stopped. The crack width was measured on concrete surface using the DNT Entwicklungs und Vetrieb digital camera with a magnification factor of 45 (Figure 4). Three samples were prepared for each crack width.

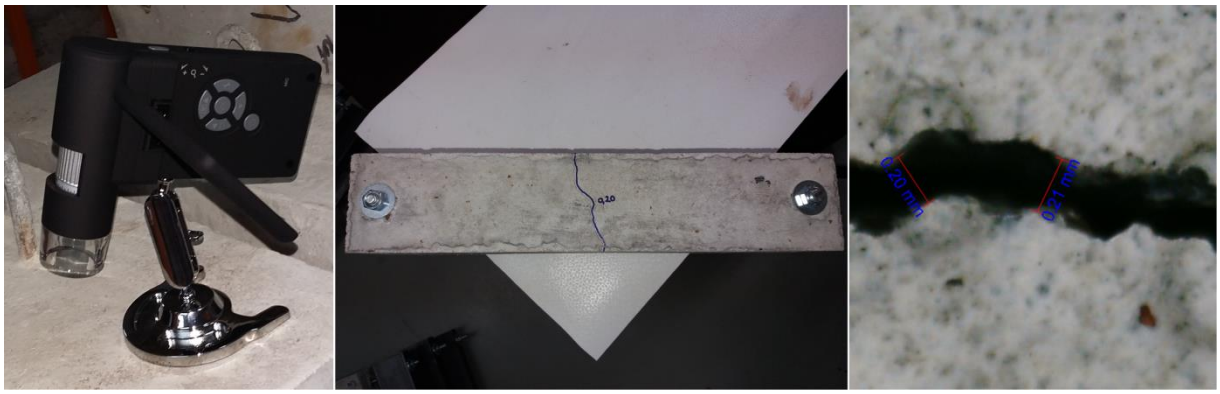

Figure 4. Crack width measurement

Subsequently, the samples with different crack widths were placed in the carbonation chamber. The accelerated carbonation tests were performed during 28 days at a CO_2 concentration of 2%, relative humidity (RH) of 65±5 % and a temperature of 20±2°C in a carbonation chamber Memmert ICH 260C (Figure 5). Measuring carbonation depth was achieved with a phenolphthalein solution sprayed on the freshly broken concrete surface according to the European standard EN 14630 [20]. Samples were broken along the longitudinal axis and then sprayed with a phenolphthalein solution. The carbonation depth was measured at every 5 mm per top/bottom side, resulting in 58 measurements (29 on each side) for every specimen.

After the samples were longitudinally broken, reinforcement bars were removed from the concrete samples and corrosion was measured. The reinforcement cross-section loss was measured using the Olympus CX41 electronic microscope, while the corrosion surface was measured using a millimetre paper.

Figure 5. Samples in the carbonation chamber

4. Experimental results and discussion

4.1. Influence of crack widths on the concrete carbonation resistance

4.1.1. Accelerated carbonation depth

The carbonation depths measured along the cracked sample surface under accelerated exposure conditions ($x_{c,ACC}$) in relation to the position of the crack are shown in Figure 6. The presented results show the mean value of three sample measurements for each crack width (w). Uncracked samples were labelled with w = 0.00 mm, while other labels define crack widths (w = 0.05–0.30 mm) measured on the sample surface. It can be seen that the impact of the crack on the carbonation depth was exerted at a length of approximately ±10 mm from the position of the crack, regardless of the crack width. For cross sections at a distance of more than 10 mm from the crack, the carbonation depths remained constant. Therefore, the effect of cracks on carbonation depth was lost after 10 mm in relation to its position. With the increase in distance from crack position, the tensile stress decreases, and outside of this zone (±10 mm in relation to the crack position) the stress is lower than concrete tensile strength.

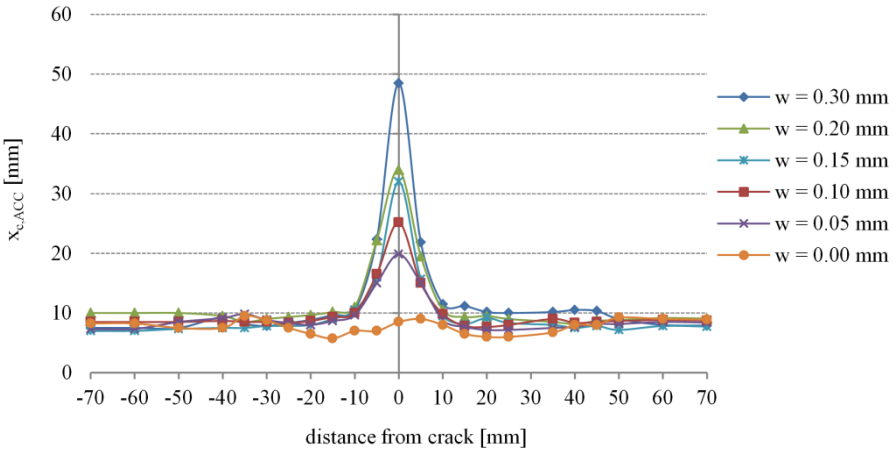

Figure 6. Carbonation depth in the tensile zone along the sample in relation to the position of the crack for different crack widths (w)

Confirmation of the previous conclusion can be seen in figures of the carbonation front (detected with a phenolphthalein test) along the samples, Figure 7. The carbonation front is fairly flat except in the narrow area around the crack, which can be defined as the crack impact area on the carbonation front. The crack impact area was approximately the same regardless of the crack width. In all cases, the cracks behaved as an additional exposed surface through which the CO_2 molecules were diffused perpendicularly to the crack wall. Even for samples with small crack widths (0.05 mm) this phenomenon was noticed, similar to other studies found in literature [13–16].

The maximum carbonation depths ($x_{c,ACC,max}$), measured at the tip of the crack, for all measured samples in relation to the crack width are shown in Figure 8. With the increase of crack width, the increase in the maximum carbonation depth can be seen. Even with the smallest crack width of 0.05 mm the maximum carbonation depth was two times higher compared with the uncracked sample. This implies that a sufficient amount of CO_2 molecules were continuously present even in the smallest crack widths due to CO_2-laden air circulation.

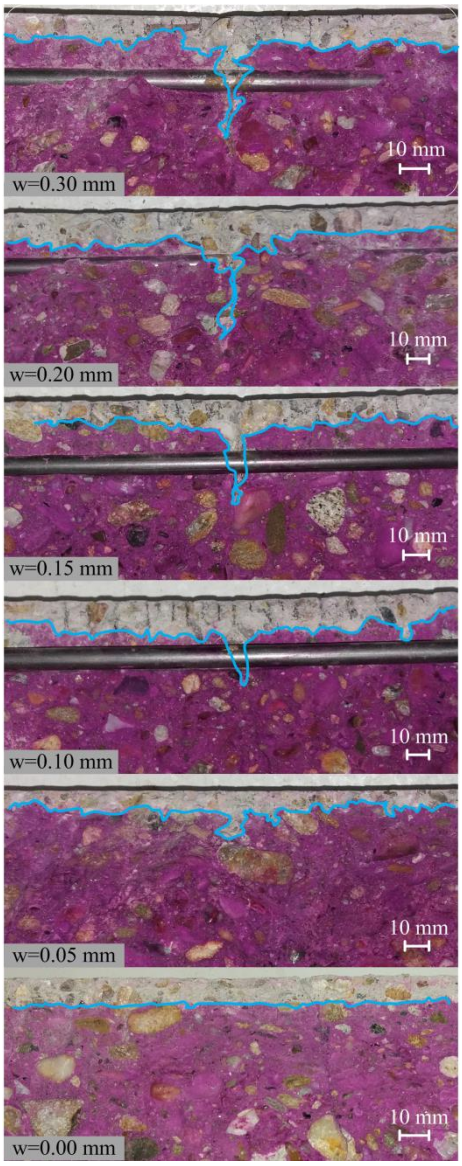

Figure 7. Carbonation front along the samples with different crack widths (*w*)

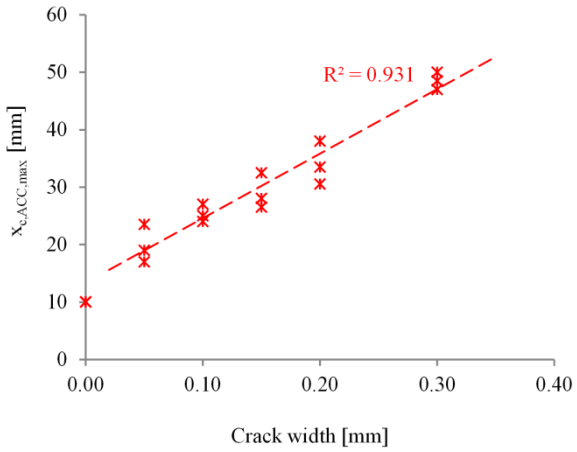

Figure 8. Maximum carbonation depth at the crack position in relation to the crack width

In case of cracked samples, a linear relationship between carbonation depth and crack width can be established (Figure 8) and determined using the least square regression method.

If we look at the standards for determining carbonation depth under natural [21] or accelerated [5,22] exposure conditions, it can be seen that the mean carbonation depth is an average value obtained at the certain length. Since cracks had a significant impact on the carbonation front only at ±10 mm in relation to their position, the length at which the average value was taken affects the mean value of the carbonation depth. In order to analyse this effect, the mean carbonation depths ($x_{c,ACC,mean}$), in relation to the crack width for the different averaging lengths, are shown in Figure 9. The averaging length represents the length at which the average value of the carbonation depth measurement was taken. The measurements were made at every 5 mm of the averaging length. The 20 mm averaging length (avg. 20 mm) was chosen based on the results presented in Figure 6, because the impact of the crack on the carbonation depth existed approximately around ±10 mm in relation to the crack position. The 50 mm averaging length (avg. 50 mm) was taken because it represents the length at which it is measured in accordance with the standard [21], while the length of 140 mm (avg. 140 mm) represents the theoretical value of the crack spacing. The mean theoretical value of crack spacing was calculated based on the recommendation for small-size reinforced beams, found in the literature [23,24].

As expected, with decreasing the averaging length, the mean carbonation depth increased. The differences for uncracked samples were negligible (up to 5%). However, for cracked samples, major differences were noticed. The differences between avg. 50 mm and avg. 20 mm compared with the avg. 140 mm increased from 15% to 49% and from 46% to 91%, respectively.

It can be seen from Figure 9 that the difference between the mean carbonation depth of cracked and uncracked samples increases linearly with the increase of the crack width, regardless of the averaging length. Even for samples with a small crack width (0.05 mm), the differences between cracked and uncracked samples were significant: 21%, 43% and 74% (depending on the averaging length). The differences increased with the decrease in the averaging length. For the avg. 140 mm the differences between cracked and uncracked samples increased along with the crack width increase from 21% to 56%. For the avg. 50 mm the differences increased compared with the avg. 140 mm and increased from 43% to 140%. The highest differences were obtained using the avg. 20 mm: the increase was from 74% to 192%.

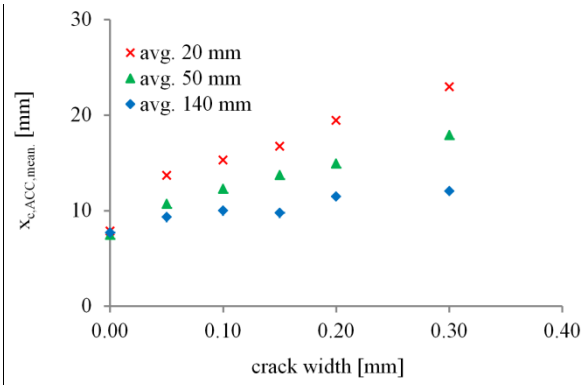

Figure 9. Mean carbonation depth in relation to the crack width

In order to evaluate the impact of these two phenomena (averaging length and the presence of cracks), it is necessary to determine the inverse effective carbonation resistance of concrete (R^{-1}_{ACC}) as a measure of concrete carbonation resistance according to the *fib* Model Code 2010 [5].

4.1.2. Inverse effective carbonation resistance of concrete

Determination of the inverse effective carbonation resistance of concrete, R^{-1}_{ACC}, is the key parameter in the *fib* Model Code 2010 [5] for service life design. It is defined with carbonation depth after 28 days at a CO_2 concentration of 2% as

$$R_{ACC}^{-1} = \left(\frac{x_c}{\tau} \right)^2 \quad (1)$$

where,

x_c measured carbonation depth [m],

τ time constant [$(s/kg/m^3)^{0.5}$], for described test conditions: $\tau = 420$.

The calculated inverse effective carbonation resistances for various averaging lengths and crack widths are presented in Table 4. Since R^{-1}_{ACC} was determined based on the mean value of the carbonation depth measurements, the same conclusions derived in the previous section for the mean carbonation depth can be applied here.

Table 4. Inverse effective carbonation resistances for various averaging lengths and crack widths

Crack width [mm]	R^{-1}_{ACC} $[10^{-11}(m^2/s)/(kg/m^3)]$					
	avg. 140 mm (1)	avg. 50 mm (2)	avg. 20 mm (3)	(2)/(1)	(3)/(2)	(3)/(1)
–	33.7	31.7	35.1	0.94	1.11	1.04
0.05	50.1	65.8	108.3	1.31	1.65	2.16
0.10	57.1	86.5	134.8	1.51	1.56	2.36
0.15	54.1	106.6	160.3	1.97	1.5	2.96
0.20	75.5	127.3	215.9	1.69	1.7	2.86
0.30	82.8	182.4	303.3	2.2	1.66	3.66

It can be seen that with the decrease in the averaging length, R^{-1}_{ACC} increased, i.e. carbonation resistance decreased. This increase was up to 3.66 in samples with a crack width of 0.30 mm. With the increase in crack width, the ratio between R^{-1}_{ACC} of cracked ($R^{-1}_{ACC,cr}$) and uncracked ($R^{-1}_{ACC,0}$) samples also increased. The cracked samples had up to 2.50 times higher R^{-1}_{ACC} than uncracked samples, when the avg. 140 mm was used. In the case of avg. 20 mm, the ratio between cracked and uncracked samples reached the value of approximately 8.50.

This practically means that in the case of samples with the crack width of 0.30 mm and the avg. 20 mm, R^{-1}_{ACC} was an order of magnitude greater than for uncracked samples.

The previous analysis showed that the averaging length and the appearance of cracks had significant influence on the increase of R^{-1}_{ACC} for accelerated exposure conditions. It is important to analyse how much it will affect carbonation depth under natural exposure conditions according to prediction model [5].

4.1.3. Prediction of the carbonation depth in natural exposure conditions

Prediction of carbonation depth under natural exposure conditions can be carried out according to the aforementioned *fib* Model Code 2010 predictions. In addition to the ambient CO_2 concentration and exposure time, this model takes into account the macro-climate conditions, curing conditions and concrete properties in explicit form:

$$x_c(t) = \sqrt{2 \cdot k_e \cdot k_c \cdot R_{NAT}^{-1} \cdot C_s \cdot t} \cdot W(t) \quad (2)$$

where,

$x_c(t)$ carbonation depth at the time t [mm],

k_e environmental function [-],

k_c execution transfer parameter [-],

R^{-1}_{NAT} natural inverse effective carbonation resistance of concrete [(mm^2/year)/(kg/m^3)],

C_s CO_2 concentration [kg/m^3],

t time of exposure [years].

$W(t)$ weather function [-].

The environmental function k_e considers the influence of RH_{real} and it was calculated using the following equation:

$$k_e = \left(\frac{1-(RH_{real}/100)^5}{1-(65/100)^5} \right)^{2.5} \quad (3)$$

In the case of concrete sheltered from rain (as it was the case) the value of the weather function was taken as $W(t) = 1$.

Execution transfer parameter k_c considers the influence of the curing period on carbonation resistance and it was calculated as

$$k_c = \left(\frac{t_c}{7} \right)^{b_c} \tag{4}$$

where,

t_c period of curing [days], for the described curing procedure: $t_c = 7$ days,

b_c regression exponent [-], according to the *fib* Model Code 2010 [5] $b_c = -0.567$.

The natural inverse effective carbonation resistance of concrete (R^{-1}_{NAT}) can be obtained from the accelerated inverse effective carbonation resistance, R^{-1}_{ACC} using the following expression:

$$R_{NAT}^{-1} = k_t \cdot R_{ACC}^{-1} + \varepsilon_t \tag{5}$$

where,

k_t regression parameter [-], average value: 1.25,

ε_t error term [(mm^2/year)/(kg/m^3)], average value: 315.5.

The possible application of the *fib* Model Code 2010 for uncracked Ordinary Portland cement concrete samples was tested and evaluated [25]. However, the appearance of cracks affects the applicability of the proposed model and its prediction accuracy. The prediction model for carbonation depth under natural exposure conditions is directly related to the natural inverse effective carbonation resistance of concrete. Therefore, it can be assumed that the carbonation depth under accelerated exposure conditions is directly related to the accelerated inverse effective carbonation resistance:

$$x_{c,ACC}(t) = \sqrt{2 \cdot k_e \cdot k_c \cdot R_{ACC}^{-1} \cdot C_s \cdot t} \cdot W(t) \tag{6}$$

If this assumption (Eq. 6) is correct, then the impact of cracks on the accuracy of the prediction model can be evaluated. Furthermore, this assumption will be analytically tested. Due to the given exposure conditions during the accelerated test (2% CO_2, RH 65% and samples protected from rain) and 7 days concrete curing, values of the parameters of the micro-climatic (k_e) and curing conditions (k_c) were set equal to 1. Application of Eq. 1 in Eq. 6 results in the following:

$$x_{c,ACC}^{calc.}\left(28\ days\right)=\sqrt{2\cdot\left(\frac{x_{c,ACC}^{meas.}}{\tau}\right)^{2}\cdot C_s^{exp}\cdot t} \tag{7}$$

The time constant τ can be replaced by the expression defined in [25]:

$$x_{c,ACC}^{calc.}\left(28\ days\right)=\sqrt{2\cdot\left(\frac{x_{c,ACC}^{meas.}}{\sqrt{2\cdot C_s^{test}\cdot 28}}\right)^{2}\cdot C_s^{exp}\cdot 28} \tag{8}$$

Since CO_2 concentrations during the accelerated test (C_s^{test}) and experiment (C_s^{exp}) were identical (2% CO_2), the following expression can be derived:

$$x_{c,ACC}^{calc.}\left(28\ days\right)=x_{c,ACC}^{meas.} \tag{9}$$

In this way, the assumption given in Eq. 6 was mathematically proven. It can be clearly seen that Eq. 6 is independent of crack occurrence which is also explicitly stated in the *fib* Model Code [5]. Having this in mind, the model proposed in the *fib* Model Code 2010 (Eq. 2) could also be used to predict carbonation depth of cracked samples.

If the same parameters for macro-climate and curing conditions were adopted, the only difference in the prediction of carbonation depth (according to Eq. 2) will be the value of R^{-1}_{ACC}. As already shown, this value will depend on the averaging length and crack width. In order to evaluate the impact of cracks on the predicted carbonation depth under natural

exposure conditions, the ratio between the calculated carbonation depths of cracked ($x_{c,NAT,cr}$) and uncracked ($x_{c,NAT,0}$) samples is shown in Figure 10.

The effect of the large increase of R^{-1}_{ACC} (in some cases for one order of magnitude) was now reduced. The ratio between the calculated carbonation depths of cracked and uncracked samples was up to three at the smallest averaging length (avg. 20 mm). This practically means that in the case of samples with a crack width of 0.30 mm, the natural carbonation depth will be three times higher than in uncracked samples. Even when larger averaging lengths were used (avg. 140 mm), the carbonation depth was up to 56% higher compared with uncracked samples.

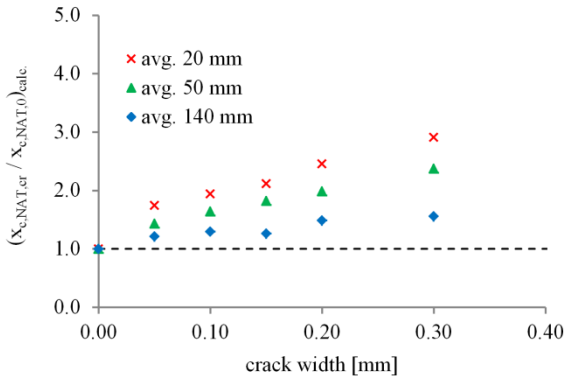

Figure 10. Ratio between calculated carbonation depths of cracked ($x_{c,NAT,cr}$) and uncracked ($x_{c,NAT,0}$) samples for various averaging lengths

In order to analyse the service life of RC structures through the thickness of the concrete cover, calculated values of R^{-1}_{ACC} were used in the semi-probabilistic design method for carbonation induced corrosion (Eq. 2). The values of parameters that define the climatic conditions and curing period were calculated according to the defined conditions as RH_{real} = 65%, t_c = 7 days, C_s = 0.00082 kg/m^3 (recommended in the *fib* Model Code 2010) and $W(t)$ = 1 (protected from rain). Calculated values of the natural carbonation depths as the function of exposure time for tested concrete are shown in Figure 11.

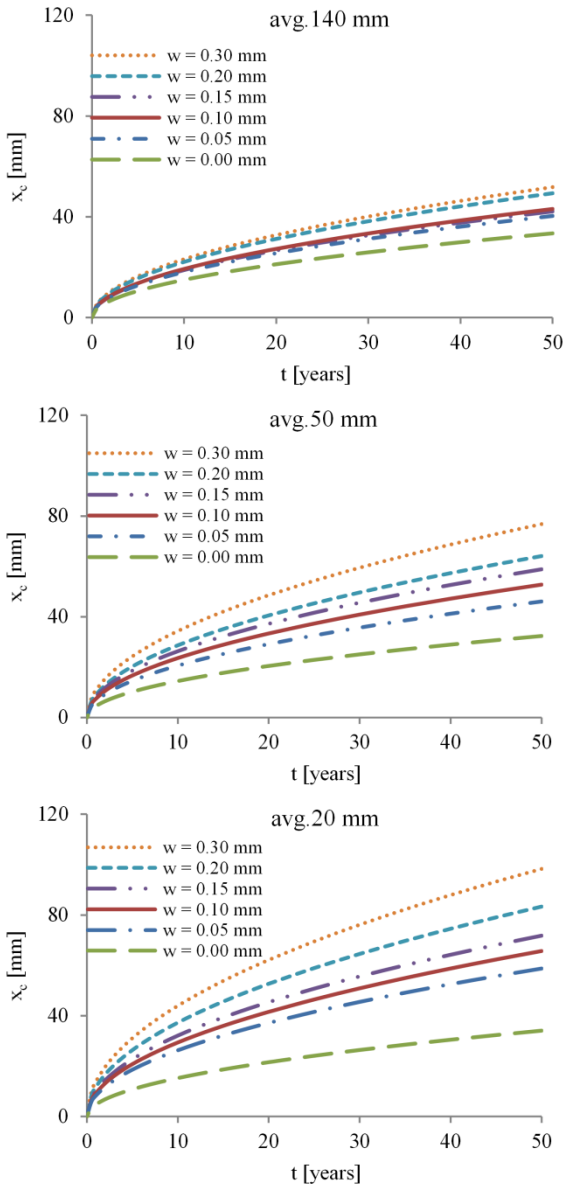

Figure 11. Carbonation depth versus duration of exposure to natural conditions for various averaging lengths and crack widths (w)

For larger averaging lengths (avg. 140 mm) the carbonation depth after 50 years of exposure (design working life for recommended Structural Class S4 according to EN 1992-1-1 [8]) ranged between 35 and 50 mm depending on the crack width. As the averaging length decreased, the carbonation depth increased. These conclusions cannot be applied to uncracked samples where the averaging length had no observable effect. The carbonation depth for w = 0.30 mm was between 80 mm (avg. 50 mm) and 100 mm (avg. 20 mm). This would

practically represent the minimum concrete cover from durability requirements of cracked RC structures made from the tested concretes. However, if corrosion occurs (which represents the start of the propagation period [26]), it is necessary to determine how cracking affects the appearance and development of corrosion, i.e. the propagation period.

4.1.4. Corrosion of reinforcement

As said previously, the concrete pore solution represents a highly alkaline environment with a pH value close to 13.5, which ensures the corrosion protection of steel reinforcement with a thin oxide layer – the passivation layer [1]. When the pH value drops below approximately 9.5, the corrosion of reinforcement can start. The presence of cracks that cross the reinforcement physically interrupts the passivation layer and induces the beginning of corrosion.

During this research, the corrosion surface of all imbedded reinforcing bars was measured using transparent plastic foil with a millimetre grid. The plastic foil was placed over the reinforcing bar, and the corrosion surface was drawn on the foil. After that, the printed foil was unwrapped and the corrosion surface was measured using a millimetre grid. The corrosion surface as the function of crack widths is shown in Figure 12.

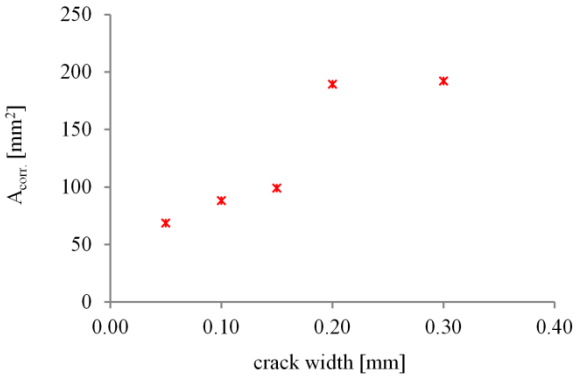

Figure 12. Corrosion surface versus crack width

In uncracked samples after 28 days of exposure, no corrosion initiation was noticed. The carbonation depth of such samples was approximately 10 mm which was lower than the

concrete cover thickness (20 mm). With the increase of crack width up to 0.15 mm the corrosion surface area increased. Between 0.15 and 0.20 mm there was a large leap in the corrosion surface area. Further crack propagation did not affect the increase in corrosion. The occurrence of local corrosion was presented in all cracked samples, Figure 13.

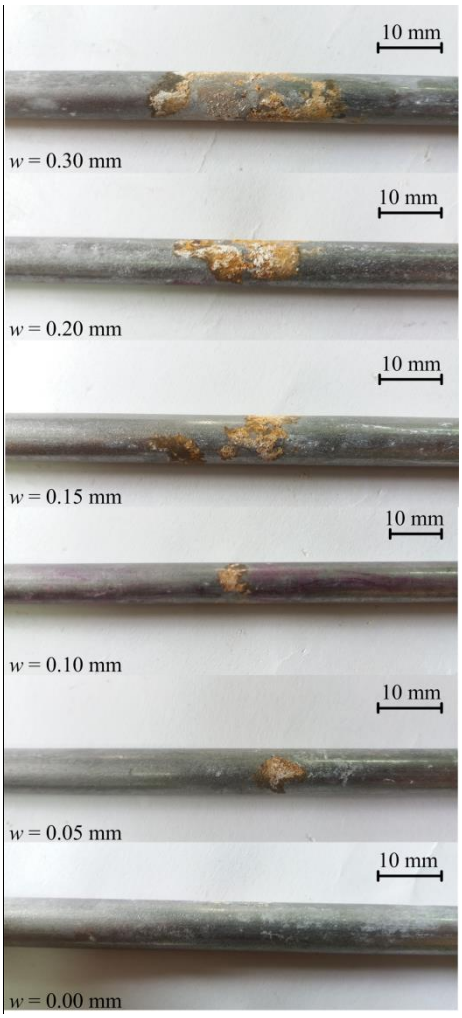

Figure 13. Reinforcement corrosion after 28 days of exposure to 2% CO_2 for different crack widths (w)

In uncracked samples, the reinforcement corrosion appeared after 168 days of exposure to accelerated conditions. Unlike cracked samples where local corrosion occurred, in uncracked samples uniform corrosion occurred when the carbonation depth reached the reinforcement bar (20 mm), Figure 14. However, when considering the consequences of the cross section

loss, there is no difference in the corrosion type – both local and uniform corrosion types lead to reduction of the reinforcement bar cross section.

Figure 14. Uniform corrosion of uncracked sample after 168 days of exposure to 2% CO_2

If this sample was found in the outdoor environment under the same exposure conditions and at the natural CO_2 concentration of 0.05% (conditions recommended in the *fib* Model Code 2010), the time required to achieve the same carbonation depth (approximately 20 mm) can be calculated using the following relation [27]:

$$\frac{x_{c,NAT}(t)}{x_{c,ACC}} = \sqrt{\frac{CO_{2,NAT}}{CO_{2,ACC}}} \cdot \left(\frac{t}{t_{ACC}}\right)^{0.5} \tag{10}$$

The calculated time under natural exposure conditions needed to achieve the same carbonation depth as in the accelerated conditions was 18.4 years. This means that in RC structures made from the tested concrete with a concrete cover of 20 mm, after 18.4 years the uniform reinforcement corrosion would occur on uncracked samples, compared with the period of 3.1 years for cracked samples (time required for corrosion occurrence at the crack position). It is important to emphasize that in case of corrosion at the crack position, local corrosion was occurred instead of uniform corrosion, Figure 13. However, taking into account that the cracks are often uniformly distributed in the maximum tension area, local corrosion would appear at the position of each crack, continuously along the reinforcing bar.

As a qualitative indicator of the reinforcing bar corrosion, corrosion surface measurements are often used. A more precise, quantitative, indicator would be the reduction of the reinforcement cross-section area. In order to determine the loss in bar cross section, the reinforcing bars were cut into thin layers (1–mm thick) and cross section surfaces were observed under an electronic microscope (Figure 15).

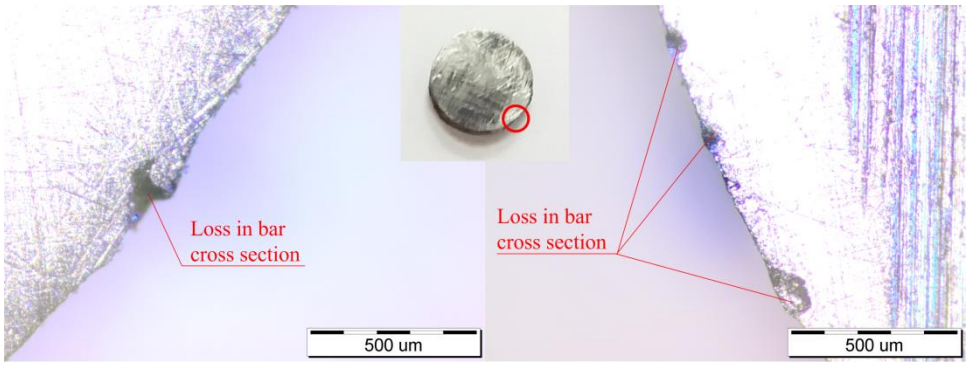

Figure 15. Measuring the loss in reinforcing bar cross section using an electronic microscope

The loss in reinforcing bar cross section ($A_{s,corr}$) as a function of crack width is shown in Figure 16. As can be seen, with the increase of crack width, the loss in cross section area also increased. Reduction in the reinforcing bar cross section was from 0.05% to 0.13%. It should be noted that this occurred after 28 days of exposure under accelerated conditions, corresponding to only 3.1 years under natural exposure conditions. After the reinforcement depassivation, corrosion can start and the reaction rate depends on the availability of oxygen and water around the reinforcing bar, which was not analysed in this study.

Since the crack represents a pathway for water and oxygen to the steel/concrete interface, the corrosion of the reinforcement will continue at the crack position over time. It is obvious that depassivation cannot be considered a serviceability limit state because, in case of RC cracked elements, reinforcement corrosion will occur rapidly after just few years.

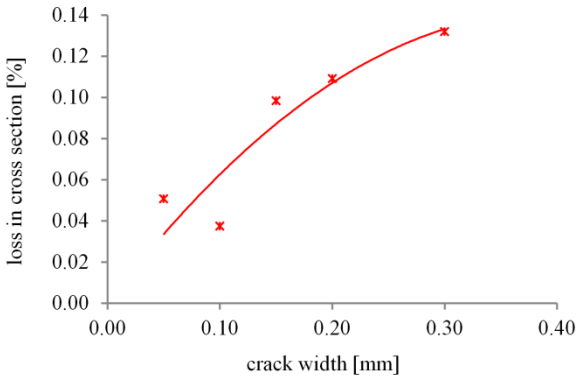

Figure 16. The loss in reinforcement cross section versus the crack width

4.2. The influence of compressive stress on the concrete carbonation resistance

The majority of research done so far in the field of loading impact on carbonation analysed the influence of cracks or tensile stresses on the concrete carbonation resistance [16–19,28] whereas only some analysed the influence of the compressive stresses [16–19]. In this part of the study, the influence of concrete compressive stress on carbonation resistance was investigated.

The obtained results regarding the carbonation depth of samples with and without cracks measured on the compressed sample surface are presented and analysed using the *fib* Model Code 2010 predictions.

4.2.1. Accelerated carbonation depth

The carbonation depths measured under accelerated exposure conditions, $x_{c,ACC}$, along the compressed side of the sample in relation to the position of the crack placed on the opposite tensioned surface are shown in Figure 17. The average carbonation depth was approximately 8 mm.

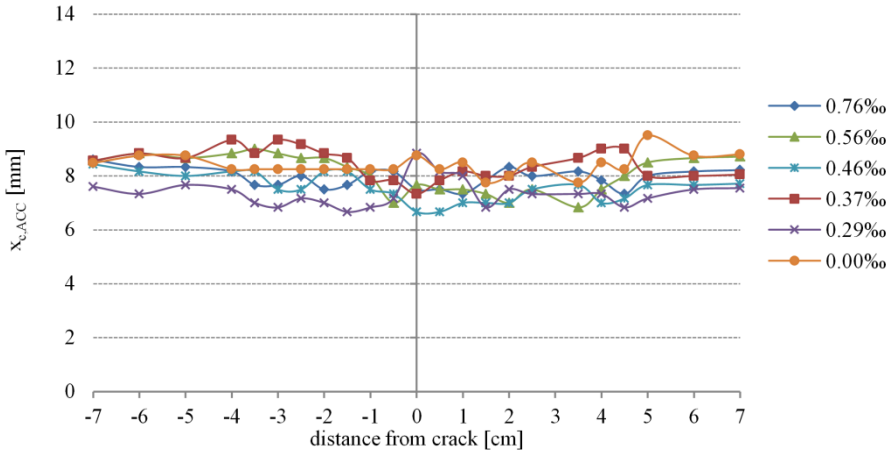

Figure 17. Carbonation depth in compressive zone along the sample in relation to the crack position

The mean carbonation depths, $x_{c,ACC,mean}$, in relation to the maximum compressive strains are shown in Figure 18. As in the case of the tensile stress zone, three averaging lengths were used: 140, 50 and 20 mm.

The calculated concrete compressive strains were up to 0.8‰, and therefore the stresses were linearly distributed in all samples. No significant difference in the carbonation depth with decreasing the averaging length was noticed. With the increase in the concrete compressive strains, there was no clear decrease in the mean carbonation depth. The maximum reduction in the carbonation depth was 15% compared with unloaded samples and it occurred at a compressive strain of 0.46‰.

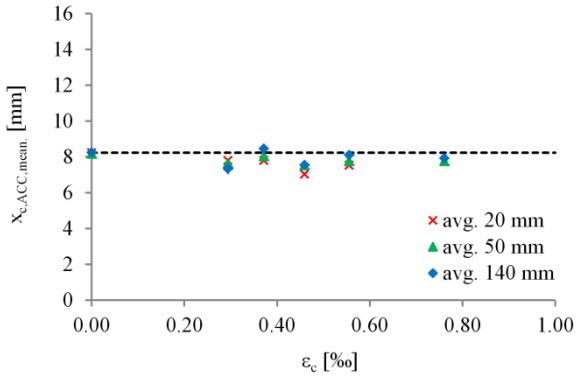

Figure 18. The mean carbonation depth in relation to the concrete compressive strain

It can be concluded that the compressive stress had a positive effect on the concrete carbonation resistance. A possible reason could be that the compression closes the micro cracks and hence reduces the degree of interconnected pores (densification of the cement-based matrix) [16,19].

Similar to the tensile stress zone, the influence of compressive stress on carbonation depth under natural exposure conditions will be analysed.

4.2.2. Prediction of carbonation depth under natural exposure conditions

The natural carbonation depth was calculated using the *fib* Model Code 2010 predictions (Eq. 2). Since R^{-1}_{ACC} was determined based on the mean value of the carbonation depth measurements, the same conclusions derived for the mean carbonation depth obtained in the previous section can be applied here. In order to analyse the effect of compressive stress on carbonation depth under natural conditions, the ratio between calculated carbonation depths of loaded ($x_{c,NAT,load}$) and non-loaded ($x_{c,NAT,0}$) samples is shown in Figure 19.

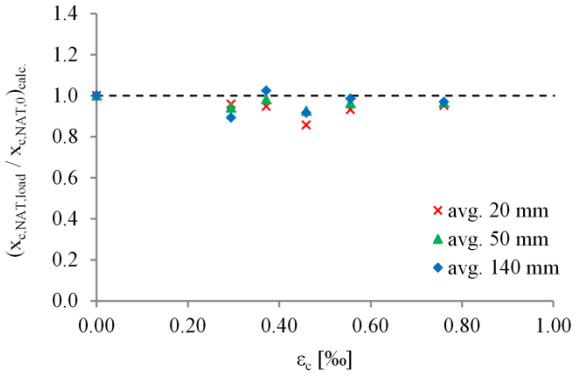

Figure 19. Ratio between calculated carbonation depths of loaded ($x_{c,NAT,load}$) and non-loaded ($x_{c,NAT,0}$) samples

No clear correlation between the carbonation depths and the compressive strain can be obtained. However, it can be seen that the compressive stress decreases the carbonation depth compared with the unloaded samples. The smallest value of this ratio was 0.86 for ε_c = 0.46‰, and 0.97 for ε_c = 0.76‰.

The previous conclusions indicate that compressive stress will affect the concrete cover depth of RC structures. In order to analyse the concrete cover depth (i.e. carbonation depth) during RC service life, calculated values of R^{-1}_{ACC} and previously defined parameters that define the climatic conditions and curing period (section 5.2.3) were used. The calculated values of the natural carbonation depths as the function of the exposure time for tested concrete are shown in Figure 20. Since it has been concluded that the averaging length did not affect the carbonation depth, only the results for avg. 50 mm are presented (which is defined by the standard EN 12390-10 [21]).

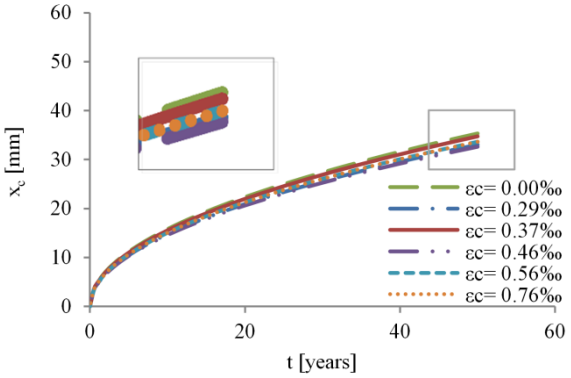

Figure 20. The carbonation depth versus time of exposure under natural exposure conditions

The carbonation depths after 50 years of exposure ranged between 33 and 35 mm. The differences between the calculated values of the carbonation depths were up to 8%. The calculated carbonation depths represent the minimum concrete cover from durability requirements of RC structures made from the tested concrete. It can be concluded that the results from the prediction model were slightly conservative – the uncracked samples had the highest value of x_c.

5. Conclusions

The main objective of this research was to analyse the influence of cracks on carbonation induced corrosion by using own experimental results and the application of available standards and novel predictions regarding carbonation depth. Based on the conducted

carbonation depth measurements on samples with and without cracks, the following conclusions can be made:

- The increase in the crack width led to the increase in the maximum carbonation depth at the tip of the crack. Even with the lowest crack width of 0.05 mm the maximum carbonation depth was two times higher compared with uncracked samples.
- The influence of cracks on the carbonation front was approximately the same (20 mm) regardless of the crack width. In all cases, the cracks behaved as an additional exposed surface through which the CO_2 molecules were diffused perpendicularly to the crack wall. Even for samples with small crack widths (0.05 mm) this phenomenon was noticed.
- With decreasing the length at which the average value of the carbonation depth was calculated (averaging length), the mean carbonation depth increased.
- The difference between the mean carbonation depth of cracked and uncracked samples increased linearly with the increase of the crack width, regardless of the averaging length.
- The ratio between the calculated carbonation depths (according to the *fib* Model Code 2010) of cracked and uncracked samples was up to three times lower. This practically means that in the case of samples with a crack width of 0.30 mm, the RC structure's service life will be approximately three times shorter compared with the uncracked samples, if the depassivation of reinforcement is assumed as an ultimate limit state.
- With the increase of crack widths up to 0.20 mm the local corrosion surface area increased, but further crack propagation did not affect the increase in corrosion surface. Also, with the increase of crack width, the loss in cross section area increased.
- With the increase in the concrete compressive strains, there was no obvious decrease in mean carbonation depth. It can be concluded that compressive stress had much less influence on carbonation resistance compared with the appearance of cracks.

It is clear that the cracks significantly influence the carbonation depth and the appearance of reinforcement corrosion. It is necessary to determine whether certain concrete types (made with fly ash, slag, recycled aggregate) affect the crack width, through self-healing process, and carbonation depth at the crack position.

Acknowledgements

English language editing was done by Nikola Tošić. His help is greatly appreciated.

Funding

This work was supported by the Ministry for Education, Science and Technology, Republic of Serbia [grant number TR36017].

Declarations of interest: none

References

[1] V.G. Papadakis, M.N. Fardis, A reaction engineering approach to the problem of concrete carbonation, Am. Inst. Chem. Eng. 35 (1989) 1639–1651.

[2] B.Q. Dong, Q.W. Qiu, J.Q. Xiang, C.J. Huang, F. Xing, N.X. Han, Y.Y. Lu, Electrochemical impedance measurement and modeling analysis of the carbonation behavior for cementititous materials, Constr. Build. Mater. 54 (2014) 558–565. doi:10.1016/j.conbuildmat.2013.12.100.

[3] V.W.Y. Tam, K. Wang, C.M. Tam, Assessing relationships among properties of demolished concrete, recycled aggregate and recycled aggregate concrete using regression analysis, J. Hazard. Mater. 152 (2008) 703–714. doi:10.1016/j.jhazmat.2007.07.061.

[4] H. Cui, W. Tang, W. Liu, Z. Dong, F. Xing, Experimental study on effects of CO2 concentrations on concrete carbonation and diffusion mechanisms, Constr. Build. Mater. 93 (2015) 522–527. doi:10.1016/j.conbuildmat.2015.06.007.

[5] fib-Model Code, Model Code 2010. Volume 2, International Federation for Structural Concrete (fib), Lausanne, Switzerland, 2010.

[6] V. Carević, I. Ignjatović, Carbonation resistance of high volume fly ash concrete with accelerated tests (in Serbian), in: XXVII Congr. Int. Symp. Res. Appl. Contemp. Achiev. Civ. Eng. F. Mater. Struct., Society for materials and structures testing of Serbia, Vrsac, Serbia, 2017: pp. 211–220.

[7] B. Pailes, Effect of Cracking on Reinforced Concrete Corrosion, ACI Spring 2018 Conv. (2018). https://www.concrete.org/education/freewebsessions/completelisting/coursepreviews.aspx?ID=51713407 (accessed March 10, 2019).

[8] Cen, EN 1992-1-1, in: CEN (Ed.), 1st ed., ISS, Belgrade, 2015.

[9] P. Schießl, Cracking of concrete and durability of concrete structures, Eur. Conf. Crack. Concr. Durab. Constr. (1988).

[10] C. Arya, F.K. Ofori-Darko, Influence of crack frequency on reinforcement corrosion in concrete, Cem. Concr. Res. 26 (1996) 345–353. doi:10.1016/S0008-8846(96)85022-8.

[11] A. Neville, Concrete: Neville's Insights and Issues, Thomas Telford Publishing, London, UK, 2006. doi:10.1680/cniai.34686.

[12] M. Sillanpää, The effect of cracking on chloride diffusion in concrete, Master Sci. Thesis. (2010) 134.

[13] S. Alahmad, A. Toumi, J. Verdier, R. François, Effect of crack opening on carbon dioxide penetration in cracked mortar samples, Mater. Struct. 42 (2009) 559–566. doi:10.1617/s11527-008-9402-x.

[14] J. Torres, C. Andrade, Influence of Crack Width on Long Term Degradation of Concrete Structures, in: C. Andrade, J. Gulikers, P. Rob (Eds.), Durab. Reinf. Concr.

from Compos. to Prot., Springer International Publishing, Delft, Netherlands, 2013: pp. 87–98. doi:10.1007/978-3-319-09921-7_9.

[15] S. Zhang, L. Zong, L. Dong, W. Zhang, Influence of Cracking on Carbonation of Cement-based Materials, Adv. Mater. Res. 261–263 (2011) 84–88. doi:10.4028/www.scientific.net/AMR.261-263.84.

[16] X.H. Wang, D. V. Val, L. Zheng, M.R. Jones, Influence of loading and cracks on carbonation of RC elements made of different concrete types, Constr. Build. Mater. 164 (2018) 12–28. doi:10.1016/j.conbuildmat.2017.12.142.

[17] Y. Ren, Q. Huang, X.L. Liu, Z.J. Tong, A model of concrete carbonation depth under the coupling effects of load and environment, Mater. Res. Innov. 19 (2015) S9-224-S9-228. doi:10.1179/1432891715Z.0000000001970.

[18] J. Tang, J. Wu, Z. Zou, A. Yue, A. Mueller, Influence of axial loading and carbonation age on the carbonation resistance of recycled aggregate concrete, Constr. Build. Mater. 173 (2018) 707–717. doi:10.1016/j.conbuildmat.2018.03.269.

[19] X. Wan, F.H. Wittmann, T. Zhao, Influence of mechanical load on service life of reinforced concrete structures under dominant influence of carbonation, Restor. Build. Monum. 17 (2011) 103–110. doi:10.1515/rbm-2011-6437.

[20] EN 14630, Products and systems for the protection and repair of concrete structures - Test methods - Determination of carbonation depth in hardened concrete by the phenolphthalein method, (2006) 8.

[21] EN12390-10, Testing hardened concrete — Part 10: Determination of the relative carbonation resistance of concrete, (2008) 21.

[22] ISO 1920-12, Tessting of concrete - Part 12: Determination of the carbonation resistance of concrete - Accelerated carbonation method, (2015) 14.

[23] A. Blagojevic, The Influence of Cracks on the Durability and Service Life of Reinforced Concrete Structures in relation to Chloride - Induced Corrosio A Look from a Different Perspective, Delft University of Technology, 2016.

[24] R. Piyasena, Crack Spacing, Crack Width, and Tension Stiffening Effect in Reinforced Concrete Beams and One-way Slabs, Griffith University, Brisbane, 2002.

[25] S. Lay, P. Schießl, LIFECON DELIVERABLE D3.2 Service Life Models, Life Cycle Manag. Concr. Infrastructures Improv. Sustain. (2003) 169.

[26] K. Tuutti, Corrosion of steel in concrete, Swedish Cement and Concrete Reasearch Institute, Stockholm, Sweden, 1982.

[27] V. Carević, I. Ignjatović, Resistance of concrete with natural and recycled aggregates on accelerated carbonation tests (in Serbian), in: Savrem. Mater. I Konstr. Sa Regul., Society for materials and structures testing of Serbia, Belgrade, Serbia, 2016: pp. 79–88.

[28] A. Castel, R. François, G. Arliguie, Effect of loading on carbonation penetration in reinforced concrete elements, Cem. Concr. Res. 29 (1999) 561–565. doi:10.1016/S0008-8846(99)00017-4.

List of tables:

List of figures: